

■ **KNEE**

Can tibial coverage in total knee replacement be reliably evaluated with three-dimensional image-based digital templating?

**A. J. Costa,
S. Lustig,
C. J. Scholes,
J-C. Balestro,
M. Fatima,
D. A. Parker**

*From Sydney
Orthopaedic Research
Institute, Chatswood,
New South Wales,
Australia*

Objectives

There remains a lack of data on the reliability of methods to estimate tibial coverage achieved during total knee replacement. In order to address this gap, the intra- and interobserver reliability of a three-dimensional (3D) digital templating method was assessed with one symmetric and one asymmetric prosthesis design.

Methods

A total of 120 template procedures were performed according to specific rotational and over-hang criteria by three observers at time zero and again two weeks later. Total and sub-region coverage were calculated and the reliability of the templating and measurement method was evaluated.

Results

Excellent intra- and interobserver reliability was observed for total coverage, when minimal component overhang (intraclass correlation coefficient (ICC) = 0.87) or no component overhang (ICC = 0.92) was permitted, regardless of rotational restrictions.

Conclusions

Measurement of tibial coverage can be reliable using the templating method described even if the rotational axis selected still has a minor influence.

Keywords: Knee, Digital templating, Reliability, Tibial coverage, Arthroplasty, Baseplate

Article focus

- We aimed to assess the intra- and interobserver reliability of a three-dimensional digital templating method based on CT reconstruction for evaluating tibial coverage in total knee replacement (TKR)
- It was hypothesised that the method was reliable, regardless of the reference axis used to align the tibial implant

Key messages

- Contemporary methods for TKR increasingly rely on digital technologies for pre-operative planning. However the reliability of these methods with respect to tibial coverage remains unknown
- This study addresses this gap in the current knowledge and describes a robust method for templating tibial coverage using CT-derived models of tibiae and various tibial components
- Further work is required to explore the optimisation between tibial coverage,

particularly of the cortical shell, and component rotation when aligning the component to the resected bone surface

Strengths and limitations

- The results are founded on robust methods of templating with immediate clinical utility and a detailed statistical analysis with respect to intra- and interobserver reliability
- Further work with a larger sample size is required to generalise to the wider population and with the vast variety of tibial components available
- The definition of 'coverage' in the present context requires more precise delineation for the assessment of the efficacy of tibial components

Introduction

Interest in templating based on three-dimensional (3D) imaging has recently emerged in parallel with the growing enthusiasm for

■ A. J. Costa, FRCSC, Orthopaedic Surgeon
 ■ S. Lustig, MD, PhD, Orthopaedic Surgeon
 ■ C. J. Scholes, PhD, Director of Research
 ■ J-C. Balestro, MD, Orthopaedic Surgeon
 ■ M. Fatima, BEng, Engineer
 ■ D. A. Parker, FRACS, Consultant Orthopaedic Surgeon
 Sydney Orthopaedic Research Institute, Chatswood, New South Wales, Australia.

Correspondence should be sent to Dr C. J. Scholes; e-mail: cscholes@sori.com.au

10.1302/2046-3758.21.2000130 \$2.00

Bone Joint Res 2013;2:1–8.
Received 22 August 2012; Accepted after revision 29 October 2012

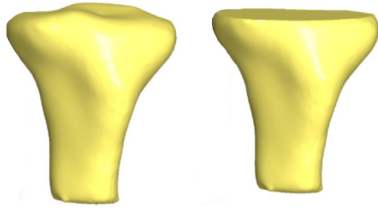


Fig. 1

Three-dimensional CT reconstructions before (left) and after resection (right).

patient-specific instrumentation. The accurate placement of components on the tibia is important to achieve maximum coverage of the resected plateau, thereby imparting good initial implant stability,¹⁻³ enhancing load transfer across the proximal tibia^{1,4-6} and decreasing the potential for implant subsidence.^{1,2,7}

In order to optimise patellofemoral tracking, a number of studies have reported rotation with reference to the medial margin of the anterior tibial tuberosity (ATT)⁸ or to the posterior condylar axis of the tibia.⁹ Many other axes of reference have been described, such as the mid-sulcus of the tibial spine,¹⁰ the distal reference axes of the foot or ankle^{9,11,12} or the femoral transepicondylar axis (TEA).^{13,14} However, the literature suffers from a lack of consensus regarding the effect of rotational alignment on coverage.¹⁵ The controversy could be related to differences in methods, but importantly the reliability of the templating and measurement method employed is consistently not reported.^{7,16-18}

Various templating methods have been used to estimate the theoretical tibial coverage afforded by different prosthesis designs.^{7,16-18} Two-dimensional (2D) tibial models created from photographed resection specimens obtained during TKR, from cadavers¹⁷ or digitised unmagnified radiographs of retrieved surgical specimens, have been described.^{2,16,19} However, the reliability of these 2D methods has never been reported, and could be questioned due to the lack of perspective and the obstruction of key anatomical landmarks when fitting the component template.

Modelling of the tibial structure in 3D has been described in cadaveric specimens,⁷ but surprisingly no recent publications have focused on digital templating of resected tibiae with contemporary modelling methods. We describe such a method based on low-dose CT imaging combined with 3D modelling. As with every new method, demonstrated reliability is a fundamental parameter before application to the clinical setting, in contrast to previous efforts.

In order to address the gap in the current literature, the purpose of this study was to assess the intra- and inter-observer reliability of a 3D digital templating method based on CT reconstruction for evaluating tibial coverage in TKR.

Our hypothesis was that the method was reliable regardless of the reference axis used to align the tibial implant.

Materials and Methods

Patients. Five patients awaiting TKR with pre-operative CT data were selected for the purposes of generating 3D tibial models. All five patients had tri-compartmental osteoarthritis and varus deformity. Three patients were male, and two were female. Their mean age was 70 years (57 to 82) and their mean body mass index was 31.8 kg/m² (21.7 to 41.7). There were three right and two left knees.

Imaging and tibial model construction. Pre-operative CT scans were performed on the affected limb for all five patients. The scan was low-dose (< 20 mSV) and comprised axial slices of the pelvis, acetabulum and femoral head, through to the bottom of the foot with 2 mm slice thickness and 512×512 pixel resolution (Aquilion, Toshiba, Japan). The CT data were acquired in Dicom format and further processed using ImageJ software (National Institutes of Health, Bethesda, Maryland), where image stacks were created before being imported into ScanIP (Simpleware LTD, Exeter, United Kingdom). In ScanIP, the axial images of the tibiae were manually segmented and an unmeshed surface of each tibia generated. The data was down-sampled to a voxel range of 3×3×3 mm to 5×5×5 mm to optimise between level of detail and computational time. After down-sampling, smoothed 3D bony surfaces of the tibia were created, which were imported into SolidWorks CAD software (Dassault Systèmes SolidWorks Corporation, Waltham, Massachusetts) for the templating process.

Tibial model preparation. After import into SolidWorks, each model was digitally resected 10 mm below the articular surface, using the lowest point on the lateral tibial plateau as a reference point. The resection was made perpendicular to the long axis of the tibia in order to simulate the tibial cut made intra-operatively during TKR (Fig. 1). Following resection, each tibial plateau was digitally marked in the axial view with two axes of rotation for reference during templating (Fig. 2). The anterior tibial tubercle axis (ATT) was defined by a line connecting the centre of the posterior cruciate attachment on the tibia and a point located at the medial third of the anterior tibial tubercle. The two points were determined for each tibia by mutual agreement between three orthopaedic surgeons (AJC, SL and JCB). The posterior condylar axis (PCA) was defined by a line drawn perpendicular to the middle of a second line connecting the most posterior points on the medial and lateral tibial condyles respectively.

Each tibia was also marked to define sub-regions of interest including the anterior, posteromedial and posterolateral regions (Fig. 3). To define these sub-regions, a medial to lateral line was drawn perpendicular to the posterior condylar axis line. This line was then shifted in the anterior-posterior direction until the widest

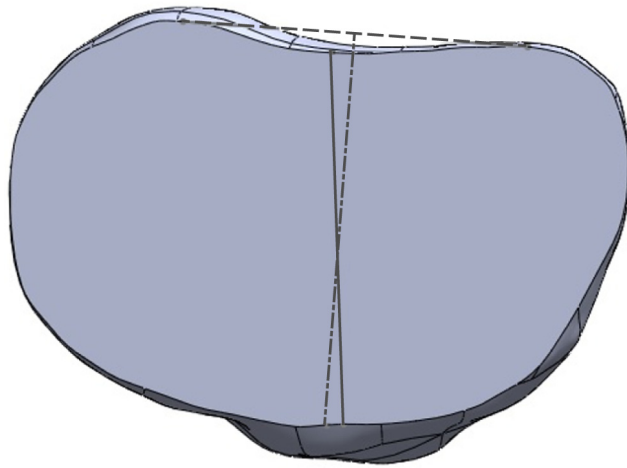


Fig. 2

Diagram showing the anterior tibial tubercle axis (ATT; solid grey line) and the posterior condylar axis (PCA; dashed line).

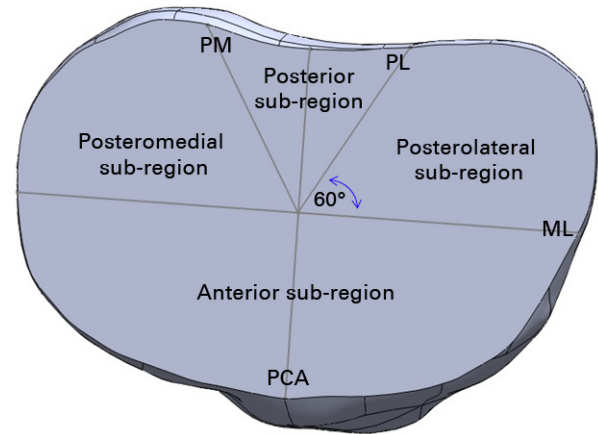


Fig. 3

Diagram showing the sub-regions of interest (PM, posteromedial line; PL, posterolateral line, ML, mediolateral line; PCA, posterior condylar axis).

medial to lateral portion of the tibia was located, which was termed the ML line. From the midpoint of the ML line, two additional lines were drawn at 60° in the posteromedial (PM line) and posterolateral directions (PL line).

Prostheses, rotation and overhang definition. Digital tibial tray templates for one symmetric design (NexGen; Zimmer, Warsaw, Indiana), and one asymmetric design (Genesis II; Smith & Nephew, Memphis, Tennessee) were obtained directly from the manufacturers, with a range of tray sizes and corresponding areas (Table I). Each tray template was marked with a line drawn perpendicular to the rotational reference notch on the anterior aspect of the tray, to standardise rotation. Tibial coverage was tested with three different rotational axes, along with two different over-hang conditions, for a total of six rotation-overhang combinations. The three rotational axes were the anterior tibial tubercle axis (ATT), posterior condylar axis (PCA) and a third axis called the best fit axis (BFA). For the BFA, the tray was free to rotate in any axis in the axial plane to obtain maximal coverage. The first over-hang condition was no-overhang (NO), where no portion of the tray template could exceed the boundary of the resected tibia (Fig. 4a). The second condition was minimal-overhang (OV), where over-hang was permitted provided it was < 2 mm from the edge of the tray to the tibial cortex and did not occur anteriorly or medially (Fig. 4b). Provided the rotation and over-hang criteria were met in each combination, observers were free to select whichever tray size deemed most appropriate and also translate the tray in the medial-lateral and anterior-posterior directions to maximise coverage.

Prosthesis templating. Three orthopaedic surgeons (AJC, SL and JCB) independently templated the five tibiae with both trays on two separate occasions. Each selected

tray was placed directly on the resected surface of the tibia in the axial plane. Rotation of the tray on the tibia was controlled to ensure that the tray was aligned with the correct rotational axis. For the best-fit condition, the tray was positioned on the resected surface in the axial plane but the surgeon was permitted to rotate the tray along any rotational axis in this plane. All six possible combinations of rotation and over-hang were templated by each surgeon for all five tibiae using both trays at time zero and again two weeks later. Adherence to rotation and over-hang restrictions was confirmed by an independent observer (MF) at the completion of each templating session. Any templated tibiae deemed unacceptable according to the described criteria were re-templated by the same surgeon.

Tibial coverage. The “Section Properties” function (within the SolidWorks software) was used to define and measure the area covered and uncovered by the tray. Tibial coverage was calculated as a proportion of the total area and for each of the sub-regions.

Statistical analysis. The intraclass correlation coefficient (ICC) and the Typical Error of Measurement (TEM, in mm^2) were used to describe both inter- and intra-observer reliability of coverage calculations.²⁰ The typical error of measurement indicates the amount of change in coverage associated with the templating and measurement method and reflects the threshold for detection of real differences between conditions. The ICC values were interpreted according to published guidelines,²¹ where an ICC value of < 0.4 indicates poor reproducibility, a value between 0.4 and 0.75 indicates fair to good reproducibility, and a value > 0.75 indicates excellent reproducibility. All statistical calculations were performed in Microsoft Excel (Microsoft, Waltham, Massachusetts).

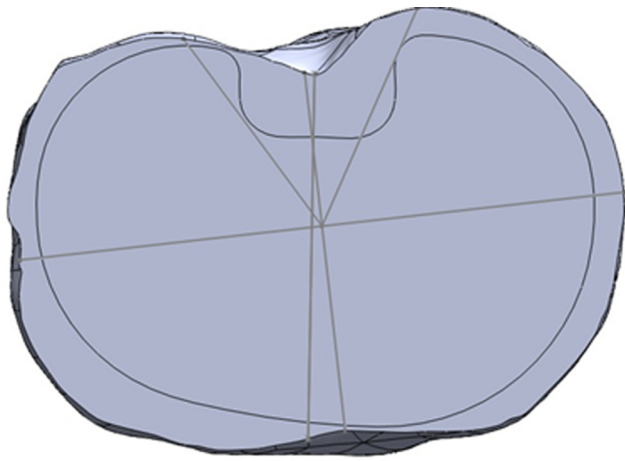


Fig. 4a

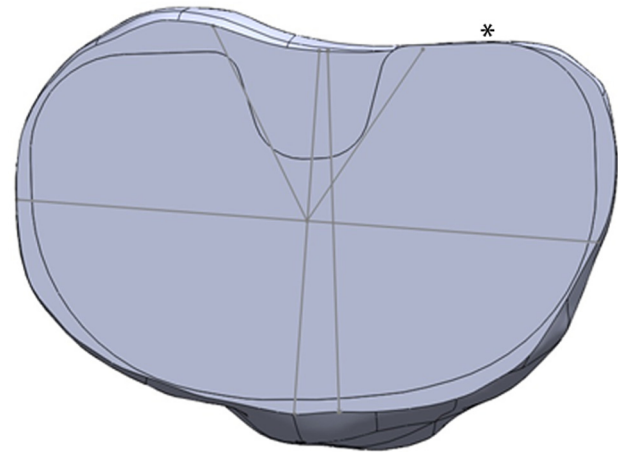


Fig. 4b

Diagrams showing the tibia template, with a) the asymmetric prosthesis aligned with the surgical axis, with no overhang permitted, and b) the symmetric prosthesis aligned with the surgical axis, with minimal posterolateral overhang permitted (*).

Results

In total, each surgeon completed 120 template procedures in accordance with the criteria and conditions described.

Excellent intra-observer reliability ($ICC \geq 0.94$; $TEM \leq 18.1 \text{ mm}^2$) was observed when the trays were aligned to the ATT axis in the NO condition (Table II). Of the sub-regions, the posteromedial region displayed lower TEM (3.4 mm^2 to 8.8 mm^2) compared with the anterior region (15.1 mm^2 to 18.1 mm^2). A similar pattern was observed for the OV condition (Table II), with excellent reliability overall ($ICC \geq 0.95$; $TEM \leq 17.2 \text{ mm}^2$) and differences in TEM between anterior (12 mm^2 to 17.2 mm^2) and posteromedial (2.9 mm^2 to 6.6 mm^2) sub-regions.

When the trays were aligned to the PCA, excellent intra-observer reliability was observed for total and sub-region coverage in the NO ($ICC \geq 0.76$; $TEM \leq 22.4 \text{ mm}^2$) and OV ($ICC \geq 0.85$; $TEM \leq 25.7 \text{ mm}^2$) conditions. Intra-observer reliability of total coverage was comparable with the ATT condition, although ICCs were lower and TEM higher for sub-region coverage in the PCA condition (Table III). Nevertheless, a similar pattern was observed across both rotation-coverage combinations, with differences in TEM between anterior and posteromedial sub-regions (Table III).

Intra-observer reliability of total coverage using the BFA to set rotation was excellent in the NO condition ($ICC 1.0$; $TEM \leq 12.1 \text{ mm}^2$) (Table IV). Similarly, sub-region coverage reliability was good to excellent ($ICC 0.58$ to 0.98 ; $TEM \leq 25.7 \text{ mm}^2$). In the OV condition, total coverage reliability was comparable ($ICC 0.73$ to 1.0), although TEM was larger than for other rotation-overhang combinations ($\leq 64.7 \text{ mm}^2$). A similar pattern was observed for sub-region reliability with ICC ranging from poor (0.25) to excellent (0.95) and higher TEM than for other conditions ($\leq 45.6 \text{ mm}^2$) (Table IV). Of note for the BFA

Table I. Number of available tibial trays and area range for each prosthesis tested

Prosthesis	Available trays (n)	Prosthesis area range (mm^2)
NexGen	10	1936 to 4093
Genesis II	8	1886 to 3900

condition was comparable reliability for the anterior and posteromedial sub-regions.

Interobserver reliability of coverage was superior when trays were aligned using the ATT axis in the NO condition ($ICC 0.94$ to 1.0 ; $TEM 8.3 \text{ mm}^2$ to 17.5 mm^2) when compared with PCA ($ICC 0.72$ to 0.94 ; $TEM 17 \text{ mm}^2$ to 54.5 mm^2) and BFA ($ICC 0.48$ to 0.98 ; $TEM 23.3 \text{ mm}^2$ to 47.1 mm^2) (Table V). In contrast, this pattern was not replicated in the OV condition (Table V), with ICC ranging from good (0.6) to excellent (1.0) for all axes and ATT total coverage displaying the highest TEM (56.2 mm^2) of any axis.

Discussion

The main finding of this study was that excellent reliability of tibial coverage can be obtained using 3D CT reconstruction and digital templating. While aligning components with the ATT axis produced the most reliable results for sub-region coverage, other axes demonstrated more variability in these measurements. Increased variability was particularly evident when no rotational control was used. Measurement of tibial coverage is overall reliable using the templating method described even if the rotational axis selected still has a minor influence. To our knowledge, this is the first study to report on the reliability of a templating and measurement method for assessing tibial coverage in TKR.

Table II. Typical error of measurement (TEM) and intraclass correlation (ICC) for intra-observer reliability of coverage with trays aligned to the anterior tibial tubercle axis (CI, confidence interval; PM, posteromedial; PL, posterolateral; Obs, observer)

	No overhang		Overhang	
	TEM (mm ²) (95% CI)	ICC (95% CI)	TEM (mm ²) (95% CI)	ICC (95% CI)
PM				
Obs1	7.8 (5.4 to 14.3)	0.99 (0.95 to 1.0)	6.6 (4.6 to 12.1)	0.99 (0.95 to 1.0)
Obs2	8.8 (6.0 to 16.0)	0.98 (0.94 to 1.0)	6.6 (4.5 to 12.0)	0.99 (0.95 to 1.0)
Obs3	3.4 (2.3 to 6.1)	1 (0.99 to 1.0)	2.9 (2.0 to 5.4)	1 (0.99 to 1.0)
PL				
Obs1	13.3 (9.2 to 24.3)	0.94 (0.78 to 0.98)	16.3 (11.2 to 29.7)	0.95 (0.82 to 0.99)
Obs2	12.1 (8.3 to 22.0)	0.97 (0.87 to 0.99)	6.7 (4.6 to 12.2)	0.99 (0.97 to 1.0)
Obs3	9.6 (6.6 to 17.5)	0.98 (0.91 to 0.99)	10.6 (7.3 to 19.3)	0.98 (0.93 to 1.0)
Anterior				
Obs1	17.1 (11.7 to 31.2)	0.98 (0.91 to 0.99)	12 (8.2 to 21.8)	0.99 (0.96 to 1.0)
Obs2	18.1 (12.4 to 33.0)	0.97 (0.9 to 0.99)	17 (11.7 to 31.0)	0.98 (0.93 to 1.0)
Obs3	15.1 (10.4 to 27.6)	0.98 (0.93 to 1.0)	17.2 (11.9 to 31.5)	0.98 (0.93 to 1.0)
Total				
Obs1	9.4 (6.5 to 17.2)	1 (0.99 to 1.0)	6.7 (4.6 to 12.3)	1 (1.0 to 1.0)
Obs2	11.2 (7.7 to 20.5)	1 (0.98 to 1.0)	7.1 (4.9 to 13.0)	1 (1.0 to 1.0)
Obs3	5.8 (4.0 to 10.6)	1 (-)	9.7 (6.6 to 17.6)	1 (0.99 to 1.0)

Table III. Typical error of measurement (TEM) and intraclass correlation (ICC) for intra-observer reliability of coverage with trays aligned to the posterior condylar axis (CI, confidence interval; PM, posteromedial; PL, posterolateral; Obs, observer)

	No overhang		Overhang	
	TEM (mm ²) (95% CI)	ICC (95% CI)	TEM (mm ²) (95% CI)	ICC (95% CI)
PM				
Obs1	10.6 (7.3 to 19.4)	0.94 (0.78 to 0.98)	11.5 (7.9 to 20.9)	0.86 (0.55 to 0.96)
Obs2	8.7 (6.0 to 15.8)	0.89 (0.61 to 0.97)	8.7 (6.0 to 15.8)	0.91 (0.69 to 0.98)
Obs3	9.4 (6.5 to 17.7)	0.89 (0.62 to 0.97)	8.3 (5.7 to 15.1)	0.92 (0.71 to 0.98)
PL				
Obs1	11.3 (7.8 to 20.6)	0.95 (0.81 to 0.99)	15.2 (10.4 to 27.7)	0.85 (0.51 to 0.96)
Obs2	10.3 (7.1 to 18.8)	0.88 (0.58 to 0.97)	12.1 (8.3 to 22.1)	0.91 (0.69 to 0.98)
Obs3	16.1 (11.1 to 29.5)	0.76 (0.29 to 0.93)	16.4 (11.3 to 30.0)	0.86 (0.55 to 0.96)
Anterior				
Obs1	22.4 (15.4 to 40.9)	0.96 (0.68 to 0.99)	25.7 (17.7 to 47.0)	0.95 (0.82 to 0.99)
Obs2	21.3 (14.7 to 38.9)	0.97 (0.89 to 0.99)	17.2 (11.8 to 31.3)	0.98 (0.91 to 0.99)
Obs3	22 (15.1 to 40.2)	0.97 (0.89 to 0.99)	16.8 (11.5 to 30.6)	0.98 (0.93 to 1.0)
Total				
Obs1	9.0 (6.2 to 16.5)	1 (0.99 to 1.0)	11.3 (7.8 to 20.6)	0.99 (0.96 to 1.0)
Obs2	8.2 (5.36 to 14.9)	1 (0.99 to 1.0)	6.5 (4.5 to 11.8)	1 (0.99 to 1.0)
Obs3	7.2 (5.0 to 13.2)	1 (0.99 to 1.0)	6.1 (4.2 to 11.2)	1 (0.99 to 1.0)

Even if digital templating could potentially revolutionise the conduct of surgical planning or sizing in the future, caution should be applied when interpreting the results if the reliability of the measurement is not well documented.^{7,16-18} Moreover, there are several disadvantages to previously reported methods, being time consuming and labour intensive, often requiring cadavers or surgical resection specimens and being prone to magnification or other measurement errors.^{2,7,16-18} A previous study compared

eight different tibial tray designs, including six symmetric and two asymmetric designs.¹⁷ However, limited details were given regarding the criteria for choosing the template size and position to calculate tibial coverage. Furthermore, no attempts were made to control for component rotation and the authors did not quantify the reliability of the technique. Others have reported differences in coverage between template designs despite repeating these methodological deficiencies. Westrich et al¹⁶ failed to

Table IV. Typical error of measurement (TEM) and intraclass correlation (ICC) for intra-observer reliability of coverage with trays aligned using the best fit condition (CI, confidence interval; PM, posteromedial; PL, posterolateral; Obs, observer)

	No overhang		Overhang	
	TEM (mm ²) (95% CI)	ICC (95% CI)	TEM (mm ²) (95% CI)	ICC (95% CI)
PM				
Obs1	15.5 (10.6 to 28.2)	0.93 (0.73 to 0.98)	45.6 (31.4 to 83.2)	0.25 (-0.42 to 0.74)
Obs2	5.4 (3.7 to 9.8)	0.98 (0.93 to 1.0)	9.1 (6.3 to 16.7)	0.94 (0.79 to 0.99)
Obs3	12.4 (8.6 to 22.7)	0.85 (0.5 to 0.96)	19.4 (13.3 to 35.4)	0.74 (0.25 to 0.93)
PL				
Obs1	16.8 (11.5 to 30.6)	0.88 (0.58 to 0.97)	13.8 (9.5 to 25.1)	0.91 (0.69 to 0.98)
Obs2	10.4 (7.2 to 19.0)	0.97 (0.87 to 0.99)	9.1 (6.2 to 16.5)	0.97 (0.87 to 0.99)
Obs3	25.7 (17.7 to 47.0)	0.58 (0 to 0.88)	25.1 (17.3 to 45.8)	0.60 (0 to 0.8)
Ant				
Obs1	16 (10.9 to 29.1)	0.98 (0.92 to 1.0)	20.7 (14.2 to 37.7)	0.93 (0.75 to 0.98)
Obs2	17.5 (12.1 to 32.0)	0.98 (0.94 to 1.0)	18.8 (12.9 to 34.3)	0.95 (0.81 to 0.99)
Obs3	24.6 (16.9 to 44.9)	0.96 (0.85 to 0.99)	37.9 (26.1 to 69.2)	0.77 (0.32 to 0.94)
Total				
Obs1	12.1 (8.4 to 22.2)	1 (0.98 to 1.0)	64.7 (44.5 to 118.1)	0.73 (0.22 to 0.92)
Obs2	5.2 (3.6 to 9.5)	1 (-)	5.7 (3.9 to 10.5)	1 (0.99 to 1.0)
Obs3	5.1 (3.5 to 9.3)	1 (-)	9.2 (6.3 to 16.8)	0.99 (0.98 to 1.0)

Table V. Typical error of measurement (TEM) and intraclass correlation (ICC) for interobserver reliability of coverage with trays aligned to the best fit axis (BFA) and the anterior tibial tubercle (ATT) and posterior condylar (PCA) axes (CI, confidence interval; PM, posteromedial; PL, posterolateral; Ant, anterior)

	No overhang		Overhang	
	TEM (mm ²) (95% CI)	ICC (95% CI)	TEM (mm ²) (95% CI)	ICC (95% CI)
ATT				
PM	8.3 (6.4 to 11.9)	0.99 (0.96 to 1.0)	14.4 (11.1 to 20.6)	0.94 (0.85 to 0.98)
PL	17.5 (13.5 to 25.0)	0.98 (0.93 to 0.99)	13.3 (10.2 to 19.0)	0.97 (0.92 to 0.99)
Ant	14.1 (10.9 to 20.2)	0.94 (0.85 to 0.98)	21.4 (16.5 to 30.7)	0.97 (0.92 to 0.99)
Total	10.1 (7.8 to 14.4)	1 (0.99 to 1.0)	56.2 (43.3 to 80.4)	0.92 (0.81 to 0.98)
PCA				
PM	17 (13.1 to 24.3)	0.74 (0.45 to 0.92)	7.4 (5.7 to 10.6)	0.94 (0.84 to 0.98)
PL	30 (23.1 to 42.9)	0.94 (0.84 to 0.98)	11.2 (8.6 to 16.0)	0.92 (0.80 to 0.98)
Ant	20.4 (15.7 to 29.1)	0.72 (0.43 to 0.91)	15.1 (11.6 to 21.6)	0.98 (0.95 to 1.0)
Total	54.5 (42.0 to 78.1)	0.87 (0.69 to 0.96)	6.6 (5.1 to 9.4)	1 (0.99 to 1.0)
BFA				
PM	30.4 (23.4 to 43.5)	0.48 (0.12 to 0.81)	24.5 (18.9 to 35.1)	0.60 (0.26 to 0.86)
PL	23.3 (17.9 to 33.3)	0.73 (0.43 to 0.91)	13.2 (10.2 to 18.9)	0.91 (0.78 to 0.97)
Ant	29.6 (22.8 to 42.4)	0.94 (0.84 to 0.98)	22.6 (17.4 to 32.4)	0.92 (0.79 to 0.98)
Total	47.1 (36.3 to 67.4)	0.93 (0.82 to 0.98)	26.4 (20.3 to 37.8)	0.95 (0.88 to 0.99)

describe the criteria for positioning the templates in the medial-lateral or anterior-posterior direction. Similarly, no attempts were made to determine the reliability of the templating and measurement technique. In another study,⁷ 3D tibial models were generated from cadaveric specimens and templated digitally with tibial trays from one symmetric and one asymmetric prosthesis design. The criteria used to position the templates in this study were defined, in contrast to previous studies, however all templating was carried out by a single surgeon and no attempt was made to assess the reliability of the templating and

measurement technique. As a result of these limitations, there remains no gold standard method to assess tibial coverage, making it difficult to compare the results. Potentially, the present study could serve this purpose for future investigations in this area.

There are several advantages to the templating and measurement method we describe compared with earlier efforts. Firstly, 3D digital tibial models were generated from CT scans. The use of CT scans over cadavers has numerous advantages in that the potential sample size is increased and demographic data more readily

available.¹⁵ Furthermore, computer digitisation of data points eliminates magnification errors and allows for manipulation in space to view the knee in the ideal orientation. A recent study reported excellent reliability using 3D-CT reconstruction to measure the position and orientation of TKR components post-operatively,²² thereby presenting a potential vehicle for future validation of the templating and measurement method described here. Further, digital templating each tibia in the present study facilitated efficiency in templating, standardised coverage calculations and ensured rotational and over-hang criteria were strictly followed. Lastly, as digital templates are now readily available from manufacturers, design changes and newer prostheses can be easily evaluated and comparisons can be made to previously tested prostheses under identical experimental conditions. In this way, labour, research costs and potential errors associated with replicating previous manual measurements, or cadaveric studies can be reduced.

Despite the advantages of our reported technique, there are also limitations of the study to note, aside from access to software to perform the templating and calculations, which may be prohibitive for some groups. First, the small sample of five tibial models is not likely to be representative of the wide variation in tibial morphology encountered by the surgeon during TKR.²³ However, templating a larger number of tibiae using the described technique is unlikely to improve the reliability reported here, although the findings would be more generalisable. Secondly, two prosthesis designs were tested, one symmetric and one asymmetric. Templating for different prosthesis designs may be less reliable, particularly if a larger spectrum of tibial models is tested. Thirdly, the concept of 'coverage' itself is not well-defined and its clinical application is hampered by a lack of consensus. Some have emphasised covering the entire resected surface,^{4,17} others have focused on optimising coverage in specific regions^{2,24-26} and still others have stressed coverage of the cortical shell.^{3,27} We demonstrated the satisfactory reliability of our method for total and sub-region surface of the total resected surface, but further studies will be required to assess cortical shell coverage. It is also important to note that we tested only two fixed rotational axes, the ATT and the PCA. There is currently no consensus with regard to the rotational alignment of the tibial component and the design might restrict the choice of rotational axis.¹⁵ The reliability of templating and measurement techniques may therefore vary considerably if other rotational axes are used.

Conclusions. In this study we demonstrated excellent reliability both within and between observers using a novel, 3D CT reconstruction-based digital templating method for assessing the total tibial coverage afforded by different prosthesis designs. The reliability of this templating method permits ready comparison of existing and future

prosthesis designs. Future studies employing this method to assess sub-region coverage should use the ATT to control for component rotation.

References

1. **Stulberg BN, Dombrowski RM, Froimson M, Easley K.** Computed tomography analysis of proximal tibial coverage. *Clin Orthop Relat Res* 1995;311:148–156.
2. **Westrich GH, Laskin RS, Haas SB, Sculco TP.** Resection specimen analysis of tibial coverage in total knee arthroplasty. *Clin Orthop Relat Res* 1994;309:163–175.
3. **Bindelglass D, Cohen J, Dorr L.** Current principles of design for cemented knees. *Techn Orthop* 1991;6:80–85.
4. **Figgie HE, Davy DT, Heiple KG, Hart RT.** Load-bearing capacity of the tibial component of the total condylar knee prosthesis: an in vitro study. *Clin Orthop Relat Res* 1984;183:288–297.
5. **Garg A, Walker PS.** The effect of the interface on the bone stresses beneath tibial components. *J Biomech* 1986;19:957–967.
6. **Goldstein SA, Wilson DL, Sonstegard DA, Matthews LS.** The mechanical properties of human tibial trabecular bone as a function of metaphyseal location. *J Biomech* 1983;16:965–969.
7. **Lemaire P, Pioletti DP, Meyer FM, Meuli R, Dörfel J, Leyvraz PF.** Tibial component positioning in total knee arthroplasty: bone coverage and extensor apparatus alignment. *Knee Surg Sports Traumatol Arthrosc* 1997;5:251–257.
8. **Insall JN, Easley ME.** *Surgery of the knee*. Vol 2. Philadelphia: Churchill Livingstone, 2001.
9. **Greenberg RL, Kenna RV, Hungerford DS, et al.** Instrumentation for total knee arthroplasty. In: Hungerford DS, Krackow KA, Kenna RV, eds. *Total knee arthroplasty: a comprehensive approach*. Baltimore: Williams and Wilkins; 1984:35.
10. **Dalury DF.** Observations of the proximal tibia in total knee arthroplasty. *Clin Orthop Relat Res* 2001;389:150–155.
11. **Insall JN.** Surgical techniques and instrumentation in total knee arthroplasty. In: Insall J, Windsor R, Scott W, Kelly M, Aglietti P, eds. *Surgery of the knee*. Second ed. Vol. 2. New York: Churchill Livingstone; 1993:739.
12. **Yoshioka Y, Siu DW, Scudamore RA, Cooke TD.** Tibial anatomy and functional axes. *J Orthop Res* 1989;7:132–137.
13. **Huddleston JI, Scott RD, Wimberly DW.** Determination of neutral tibial rotational alignment in rotating platform TKA. *Clin Orthop Relat Res* 2005;440:101–106.
14. **Barrack RL, Schrader T, Bertot AJ, Wolfe MW, Myers L.** Component rotation and anterior knee pain after total knee arthroplasty. *Clin Orthop Relat Res* 2001;392:46–55.
15. **Bonnin MP, Saffarini M, Mercier PE, Laurent JR, Carrillon Y.** Is the anterior tibial tuberosity a reliable rotational landmark for the tibial component in total knee arthroplasty? *J Arthroplasty* 2011;26:260–267.
16. **Westrich GH, Agulnick MA, Laskin RS, Haas SB, Sculco TP.** Current analysis of tibial coverage in total knee arthroplasty. *The Knee* 1997;4:87–91.
17. **Incavo SJ, Ronchetti PJ, Howe JG, Tranowski JP.** Tibial plateau coverage in total knee arthroplasty. *Clin Orthop Relat Res* 1994;299:81–85.
18. **Wevers HW, Simurda M, Griffin M, Tarrel J.** Improved fit by asymmetric tibial prosthesis for total knee arthroplasty. *Med Eng Phys* 1994;16:297–300.
19. **Westrich GH, Haas SB, Insall JN, Frachie A.** Resection specimen analysis of proximal tibial anatomy based on 100 total knee arthroplasty specimens. *J Arthroplasty* 1995;10:47–51.
20. **Hopkins WG.** Measures of reliability in sports medicine and science. *Sports Med* 2000;30:1–15.
21. **Rosner B.** *Fundamentals in biostatistics*. Belmont: Duxbury Press, 2005.
22. **Hirschmann MT, Konala P, Amsler F, et al.** The position and orientation of total knee replacement components. *J Bone Joint Surg [Br]* 2011;93-B:629–633.
23. **Hashemi J, Chandrashekar N, Gill B, et al.** The geometry of the tibial plateau and its influence on the biomechanics of the tibiofemoral joint. *J Bone Joint Surg [Am]* 2008;90-A:2724–2734.
24. **Alexiades M, Sands A, Craig SM, Scott WN.** Management of selected problems in revision knee arthroplasty. *Orthop Clin North Am* 1989;20:211–219.
25. **Bloebaum RD, Bachus KN, Mitchell W, Hoffman G, Hofmann AA.** Analysis of the bone surface area in resected tibia. Implications in tibial component subsidence and fixation. *Clin Orthop Relat Res* 1994;309:2–10.
26. **Walker PS, Greene D, Reilly D, et al.** Fixation of tibial components of knee prostheses. *J Bone Joint Surg [Am]* 1981;63-A:258–267.
27. **Bartel DL, Burstein AH, Santaviceca EA, Insall JN.** Performance of the tibial component in total knee replacement. *J Bone Joint Surg [Am]* 1982;64-A:1026–1033.

Funding statement:

- Financial support for this study was provided by the Sydney Orthopaedic Research Institute. Patient imaging was originally funded by Stryker South Pacific for an unrelated study.

Author contributions:

- A. J. Costa: Data collection, Writing the paper
- S. Lustig: Data collection, Writing the paper
- C. J. Scholes: Concept development, Statistical analysis, Writing the paper
- J-C. Balestro: Data collection, Manuscript approval
- M. Fatima: Data collection, Data analysis, Writing the paper
- D. A. Parker: Concept development, Manuscript approval

ICMJE Conflict of Interest:

- None declared

©2013 British Editorial Society of Bone and Joint Surgery. This is an open-access article distributed under the terms of the Creative Commons Attributions licence, which permits unrestricted use, distribution, and reproduction in any medium, but not for commercial gain, provided the original author and source are credited.